RSC Advances

PAPER

View Article Online
View Journal | View Issue

Cite this: *RSC Adv.*, 2025, **15**, 252

SERS of nitro group compounds for sensing of explosives

Nazar Mazur, * Volodymyr Dzhagan, Olga Kapush, Oksana Isaieva, Petro Demydov, Vitalii Lytvyn, Volodymyr Chegel, Oleksandr Kukla and Volodymyr Yukhymchuk

Detecting small concentrations of nitro-compounds *via* surface-enhanced Raman spectroscopy (SERS) is reported. In particular, explosive analogues, such as 4-nitrophenol, 1-nitronaphthalene, and 5-nitroisoquinoline, and an explosive material (picric acid) are investigated and prepared by measurements using two different methods. One method involved mixing the analyte with plasmonic silver nanoparticles (Ag NPs) in a solution, followed by subsequent drop-casting of the mixture onto a silicon substrate. In the second method, the analyte solution was drop-casted onto SERS substrates formed by annealing of thin Ag films deposited over self-assembled layers of SiO_2 spheres. Both approaches allowed for the SERS detection of analyte concentrations down to 10^{-4}–10^{-7} M. Furthermore, the possible reasons for the different enhancements of the above analytes as well as their differences in the liquid (drop) and dried states are discussed.

Received 11th October 2024
Accepted 13th December 2024

DOI: 10.1039/d4ra07309f

rsc.li/rsc-advances

Introduction

Over the past few decades, researchers have developed a number of methods to accurately and efficiently detect explosives. They generally fall into two categories. One is the bulk explosive detection technology, including X-ray imaging,[1] nuclear quadrupole resonance,[2] and neutron activation.[3] This category is suitable mainly for the detection of large quantities of explosive material hidden from visual detection. Another type is the technologies for detecting traces of explosive substances, which include ion mobility spectrometry,[4] electrochemical detection,[5] colorimetric analysis,[6] mass spectrometry,[7] fluorescence,[8] Raman spectroscopy,[9] terahertz spectroscopy,[10] and localized surface plasmon resonance.[11,12]

The development of a technique for detecting explosive materials based on surface-enhanced Raman spectroscopy (SERS) is of great relevance from the viewpoint of countering potential threats in the field of national and global security. SERS stands out as a highly promising method for ultrasensitive chemical analysis of both organic[13–19] and inorganic[16,20,21] substances, bringing it closer to practical utilization.[13,14,16,22–25] The noble metal nanostructures with localized surface plasmon resonance (LSPR) that are capable of amplifying Raman scattering from the analyte molecule are commonly referred to as "SERS substrates". Raman spectroscopy serves as a highly efficient and non-invasive technique for the rapid detection of diverse materials by analysing their vibrational spectra.[26] The role of SERS is to enhance weak Raman signals. In contrast to conventional Raman spectroscopy, SERS enables the detection of molecules even in minute concentrations in solutions or when deposited onto nanostructured noble metal films.[27] This technique can be used to detect contamination in air,[28] soils,[29] and water sources,[30] including chemical substances that are components or decomposition products of various types of explosives that may threaten the environment and human health. Low concentration detection, versatility in the types of analytes, and non-destructive analysis are the advantages of SERS compared with other techniques described above.

Several studies have considered the application of SERS technology in the field of detection of explosive substances in the past.[31–46] Hakonen *et al.*[32] focused on the portability of the SERS detector and discussed in detail the development of SERS technology in the field of detection of explosives and chemical reagents. This study[33] mainly summarized the principle of SERS, colloidal nanoparticles of the SERS substrate in solution or surface deposition nanostructure, and the application of SERS technology for the detection of explosive substances in water and the atmosphere. However, in the above SERS reviews, little attention has been paid to SERS substrates.

In this work, we developed efficient SERS substrates based on silica (SiO_2) nanospheres, synthesized by a straightforward route based on the modified Stöbel method,[47] self-assembled into large-area ordered arrays on a substrate, and subsequently covered with a thin Ag layer. We showed recently that such SERS substrates demonstrate very high performance, enabling the detection of standard dye analytes (Rhodamine 6G) down to 10^{-13} M.[48] Another method of detecting explosives materials, which was used in this work, for comparison, was

V. Ye. Lashkaryov Institute of Semiconductor Physics, National Academy of Sciences of Ukraine, 41 Nauky Avenue, 03028 Kyiv, Ukraine. E-mail: nazarmazur1994@gmail.com

mixing analytes with colloidal Ag nanoparticles in solution, which was also previously successfully tested by us on dyes and biomolecules.[49] As explosive analogues, we investigated several nitro-compounds: 4-nitrophenol (4-NP), 1-nitronaphthalene (1-NN), and 5-nitroisoquinoline (5-NI). Additionally, we used 2,4,6-trinitrophenol (also known as picric acid) as an explosive material to investigate.

Experimental

Materials

All the chemical reagents used in our experiment were of analytical grade and were used as received without further purification. All reagents used for synthesis were supplied by Sigma-Aldrich.

For silver nanoparticles, solution was prepared from silver nitrate solution ($AgNO_3$, 0.005 M), sodium citrate ($C(CH_2COONa)_2COONa$, 1%) and deionized (DI) water.

For SiO_2 nanospheres, a precursor solution was prepared from tetraethyl orthosilicate (TEOS: $Si(OC_2H_5)_4$, technical grade, 97%), and ethanol (96%) was adopted as the precursor solvent. Ammonia (NH_3, 25%) solution was used to increase the pH to promote gelation. H_2O was distilled and deionized.

Synthesis

Synthesis of silver nanoparticles (Ag NPs) was performed by mixing $AgNO_3$ (25 ml) and sodium citrate (5 ml) with DI water (100 ml) under stirring. The obtained solution was kept in a dark place for 24 hours for the stabilization of nanoparticles. Synthesis is well known and used in literature.[50]

Fine amorphous SiO_2 nanoparticles with a narrow size distribution were prepared by applying a sol–gel approach. In particular, it is based on the Stöber method with certain changes. A detailed description of the synthesis is provided in ref. 47.

To fabricate the SERS substrates, SiO_2 NPs were drop-casted on a Si substrate and dried. Then, by applying the thermal evaporation method, a thin Ag layer (of nominal thickness of 15 nm) was deposited, and the obtained structure was annealed in an inert atmosphere at 300 °C for 10 min.

The morphology of the bare SiO_2 and Ag-covered SiO_2 nanosphere films was studied using scanning electron microscopy (SEM, Tescan Mira 3 MLU). An Ag layer with a thickness of 15 nm was deposited by thermal evaporation in a vacuum of 2×10^{-3} Pa. Optical absorption spectra were obtained using a StellarNet Silver Nova 25 BWI6 spectrometer. Raman spectra were excited with a 457 nm solid-state laser and acquired using a single-stage spectrometer MDR-23 (LOMO) equipped with a cooled CCD detector (Andor iDus 420, UK). The laser power density of the samples was less than 10^3 W cm^{-2} to preclude any thermal or photo-induced modification of the samples. A spectral resolution of 4 cm^{-1} was determined from the Si phonon peak width of a single-crystal Si substrate. The Si phonon peak position of 520.5 cm^{-1} was used as a reference to determine the position of the peaks in the Raman/SERS spectra of the analyte.

In the case of using Ag NPs, the water solutions of analytes were mixed with colloidal Ag NPs in solution and drop-casted on a Si substrate. In other cases, the analytes were drop-casted on SERS substrates. Measurements of Raman spectra were performed both from dropped solutions and after drying.

Results and discussion

Optical characterization of Ag NP and SERS substrates

Fig. 1a depicts the optical absorption spectra of colloidal AgNPs measured in a solution in a cuvette. We can observe that a localized surface plasmon resonance (LSPR) band at 425 nm (Fig. 1a) is characteristic of Ag NPs of several tens of nm in diameter.[51,52]

Optical reflection spectra of obtained SiO_2 spheres covered with 15 nm of Ag film (by applying the thermal evaporation method) on glass and Si substrates (Fig. 1b) were measured in reflection geometry. Spectra exhibit a plasmon band in the same spectral range as for the colloidal NPs, ~420–425 nm, enabling comparison of the SERS performance of these two types of plasmonic structures. The detailed SEM characterization of the SERS substrates was performed by us in ref. 48; thus, Fig. 2 shows only the representative images of densely packed bare SiO_2 spheres with an average size of ~200 nm (a), the

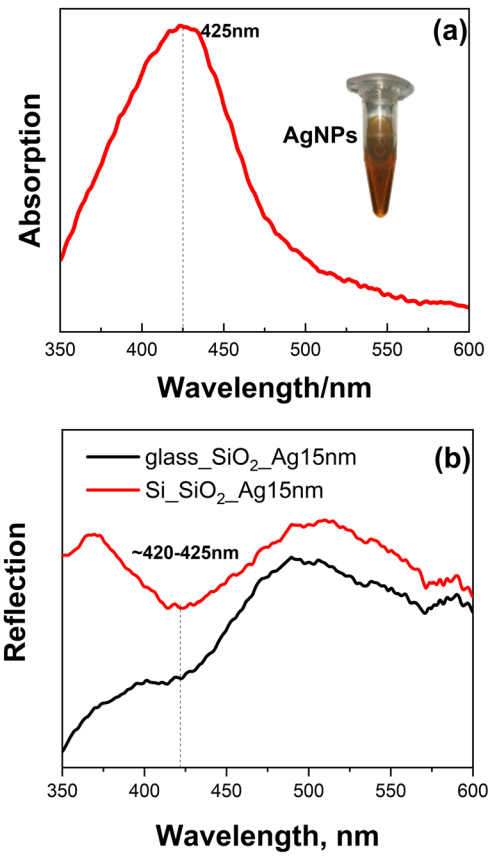

Fig. 1 Optical absorption spectra of (a) colloidal Ag NPs and (b) reflection spectra of SiO_2 nanospheres covered with 15 nm Ag film. Inset: photo of the synthesized colloidal Ag NPs (a).

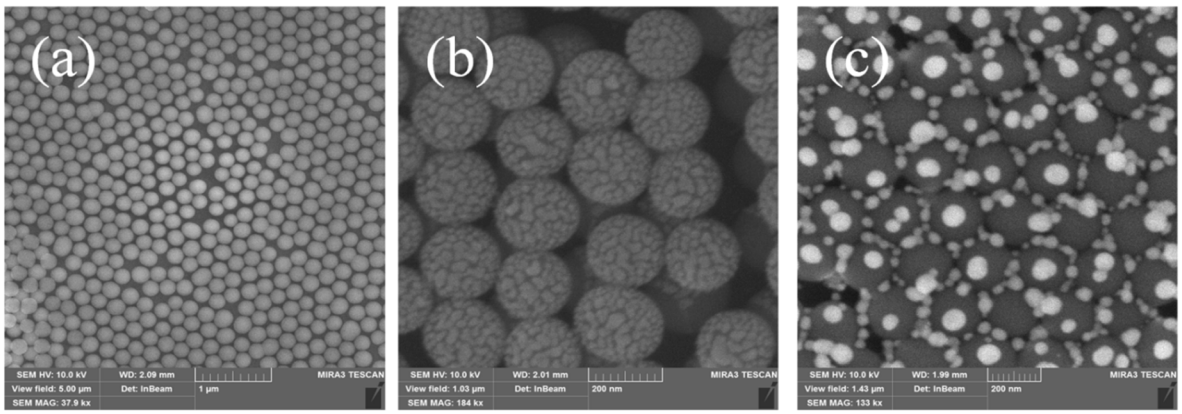

Fig. 2 SEM image of the self-assembled SiO_2 nanospheres on Si substrate (a), spheres covered with 15 nm Ag layer (b), and annealed at 300 °C (c).

spheres overcoated with 15 nm of thermally evaporated Ag, (b) and the final morphology after annealing at 300 °C (c).

Raman scattering study

The laser wavelength $\lambda_{exc} = 457$ nm was resonant with LSPR, so it was chosen for the SERS study. Raman spectra of the initial powders of explosive analogue materials were measured with the same λ_{exc}. Then, the powders were dissolved in water at different concentrations to determine the lowest concentration of these compounds, which could be detected using standard Raman spectroscopy.

The solutions were drop-casted onto the Si substrate and measured from both the drop and after the solutions were dried.

As shown in Fig. 3a–d, all analytes can be reliably detected down to 10^{-2}–10^{-3} M (the intensity is comparable to the powder samples), but after decreasing the concentration by another order of magnitude, no Raman peaks could be observed.

For all investigated analytes, the spectra of their water solutions (with different concentrations) have the same Raman bands (with the same wavenumber position) as their powder analogues; only a slight upside shift is observed for the 4-NP sample. Powder samples were measured using a neutral filter to avoid saturation of the CCD detector. Picric acid was available only in the solutions.

Therefore, the next step was to detect lower concentrations of the above analytes using the SERS technique.

SERS study

Solutions with silver nanoparticles. Investigated water solutions of the analyte of certain concentrations were mixed with Ag NPs in a 1 : 1 ratio and dropped on a Si substrate. Fig. 4 shows the SERS spectra of these samples in the form of solutions (immediately after the drop deposition) and in the dried state (*i.e.* after the solvent evaporated from the drop).

To exclude the possible contribution of the molecules belonging to the colloidal Ag NPs in the SERS spectra of our samples, the spectrum of the pure Ag NP sample is shown by an orange curve in each graph in Fig. 4(a–e). The black curve on each graph corresponds to the reference sample – pure analyte (*i.e.* without Ag NPs).

For 1-NN (Fig. 4a) after adding Ag NPs, we observe the deterioration of analyte intensity (only 1336 and 1567 cm^{-1} bands of 1-NN can be observed in the figure) even for 10^{-2} M despite the strong Raman features observed for the analyte solution without Ag NPs (black curve). There are different reasons responsible for the weakening of the Raman signal in the case of a mixed solution with Ag NPs. For example, the unfavourable pH level of colloid destroys or modifies molecular structure or polarizability and therefore influences (decreases) the Raman scattering cross section.

After mixing 4-NP with Ag NPs, the intensity of the bands increases, and we can identify 4-NP features down to 10^{-5} M (Fig. 4b).

For sample 5-NI after mixing with Ag NPs (Fig. 4c and d – spectra of dropped and dried solutions), analyte peaks for 10^{-5}–10^{-6} M concentrations can be detected (for measurements of dried samples). However, for a dropped solution, peaks of 5-NI are present on the spectra only down to 10^{-4} M. Such behaviour was already reported by us for other analytes, where we had lower concentrations detected for dried samples (R6G in ref. 48 and lysozyme and salicylic acid in ref. 53) or for dropped ones (R6G in ref. 54). This can be explained by applying the mechanisms of analyte drying on a particular type of SERS substrate (or in a mixture with colloidal Ag NPs) and concomitantly entrapping different analytes in the hot spots. Further factors could be different adsorption geometry and a different contribution of the chemical enhancement in the solution and the dry form.

After mixing picric acid with Ag NPs, we can observe SERS peeks of analyte down to 10^{-6} M (Fig. 4e), which is three orders of magnitude better than Raman detection without Ag NPs (Fig. 3d).

Solutions on SiO_2 nanospheres covered with a 15 nm Ag layer. It is well known that the major contribution to the SERS intensity is made by the "hot spots" – few-nm gaps between neighbouring plasmonic NPs or sharp edges of other

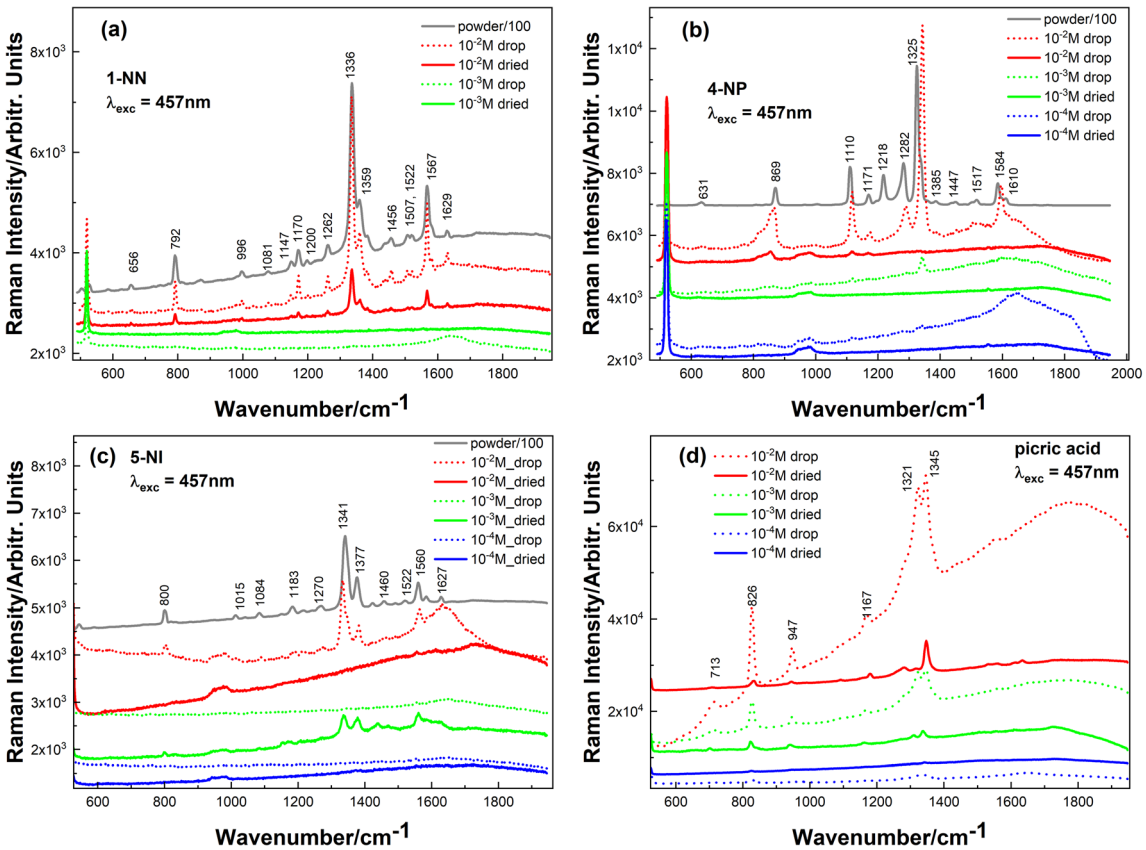

Fig. 3 Raman spectra of (a) 1-NN, (b) 4-NP, (c) 5-NI and (d) picric acid. Grey curves-powder spectra, dotted curves-solution of different concentration, solid ones-dried solutions.

nanostructured noble metal morphologies.[55,56] In the case of colloidal NPs described above, the formation can occur between two or many NPs due to the partial aggregation of NPs. The reasons for different aggregations can be the weakening of colloidal stability due to changes in pH caused by the addition of analyte molecules, or electrostatic interaction between the analyte molecules and the NPs (or its ligand shell).[57,58] The aggregation can be additionally stimulated by adding cations or anions, in particular, by dissolving salts, such as NaCl.[59,60] The advantage of colloidal NPs is that a large number of hot spots can be created at once, but the disadvantage is that the formation of hot spots in colloidal systems is not a well controllable and reproducible process.[61] Therefore, great efforts of the researchers are put towards developing pre-determined morphologies capable of the generation of large areal or spatial density of hot spots.[62–69] In this work, we used the kind of SERS substrates recently developed by us, which proved to be efficient for dye analytes and biomolecules.[48] Despite the relatively straightforward and cheap fabrication procedure, the resulting morphology reveals a large area of highly homogeneous hot spots between metal NPs situated in the dips (between SiO_2 spheres) intended for the localization of the analyte exactly in the hot spots (Fig. 2b). The metal NPs are formed by self-assembling during thermal annealing of the thin (15 nm) continuous Ag film deposited over the layer of SiO_2 nanospheres (Fig. 2c).

For the SERS study of the explosive compounds, solutions of various concentrations were deposited on these SERS substrates by drop casting. The results are presented in Fig. 5 for measurements performed on the drop of the solution immediately after its deposition (dotted curves) and after the solution was dried (solid curves).

The most pronounced difference in the SERS performance of the SERS substrates compared to mixing with colloidal Ag NPs was observed in the case of 1-NN molecules. Here, we can observe that 1-NN with a concentration down to 10^{-4} M can be identified (Fig. 5a), while only 10^{-2} M could be measured without SERS (Fig. 3a), and using colloidal Ag NPs surprisingly gave no Raman signal even at 10^{-2} M concentration (Fig. 4a).

As depicted in Fig. 5b, we observe that a 10^{-5} M concentration of 4-NP can be reliably detected, which is the same order of magnitude for colloidal Ag NPs (in the case of measuring a dropped solution of the same concentration, Raman peaks disappeared after drying (Fig. 5b)).

The best sensitivity among the studied explosive-like compounds was achieved using SERS substrates for the 5-NI molecule. Fig. 5c shows the possibility of measuring even a 10^{-7} M concentration of 5-NI in the solution state (drop), while only 10^{-4} M was detected with colloidal Ag NPs (Fig. 4c).

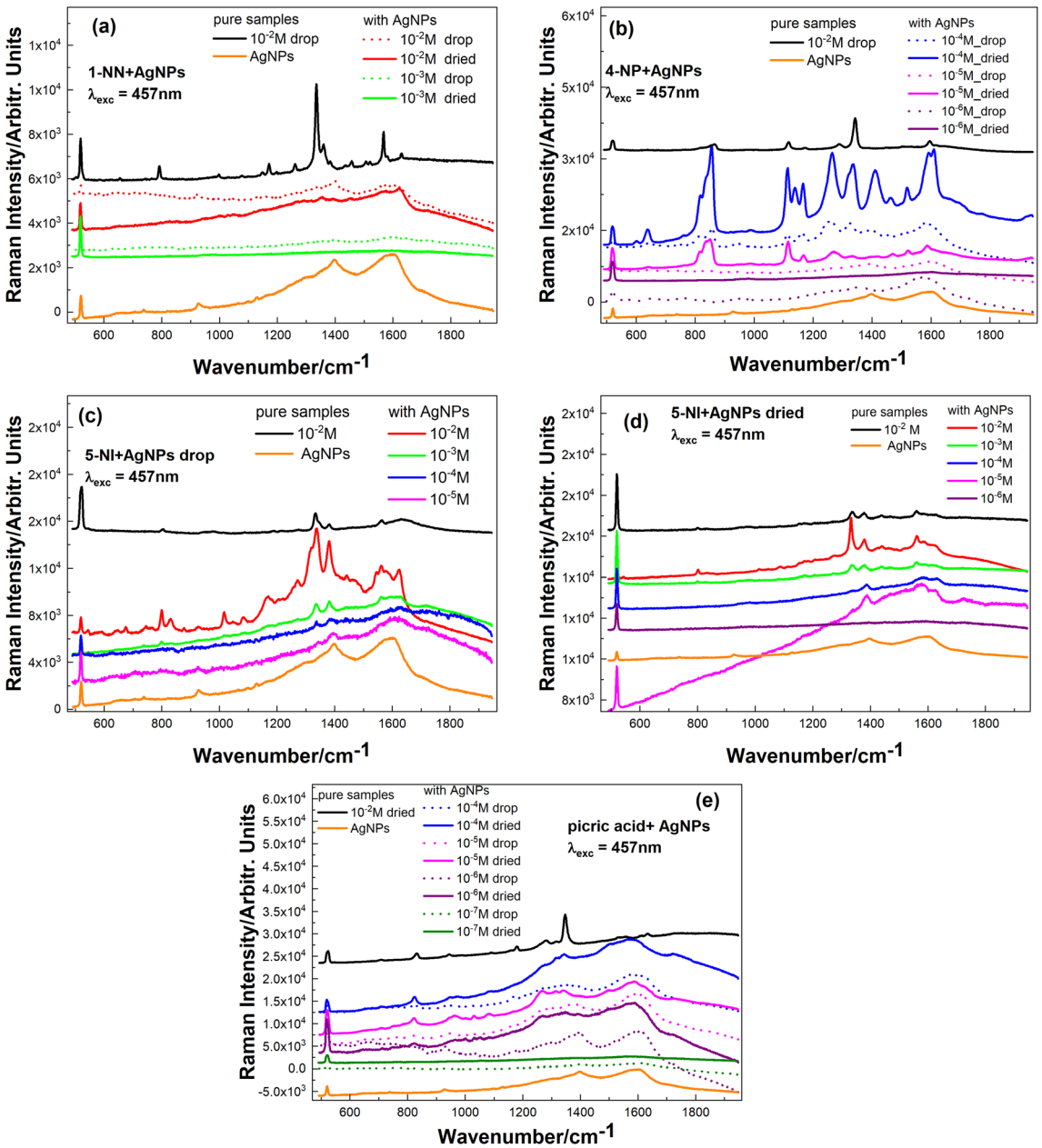

Fig. 4 SERS spectra of the investigated samples mixed in solution with Ag NPs: (a) 1-NN, (b) 4-NP, (c) 5-NI drop, (d) 5-NI dried, and (e) picric acid. The orange curve shows the spectrum of the bare Ag NP sample.

The behavior of the picric acid spectra is interesting. Although the colloidal Ag NPs were detected down to 10^{-6} M (Fig. 4e), on the SERS substrate, their peaks were recognizable down to 10^{-5} M (Fig. 5d). Moreover, two additional observations are worth noting: (i) the spectrum of 10^{-5} M is better than 10^{-4} M (the same behavior was demonstrated by us in ref. 48 with spectra of Rhodamine 6G and was explained that the number of analyte molecules became comparable to (or even smaller than) the number of hot spots), and (ii) in the case of 10^{-5} M, spectrum of dried solution is much better than that of the drop.

A comparative analysis of detected concentration levels using different approaches to sample investigation is summarized in Table 1. As we can see, for samples drop-casted on SERS substrates, on average, higher sensitivity could be achieved (at least 2–3 orders of magnitude for 1-NN and 5-NI, and the same order for 4-NP) compared to mixing the same solutions with colloidal Ag NPs, except only for picric acid, a smaller concentration of which is detected when mixing with Ag NPs. The smallest concentration detected for 5-NI is 10^{-7} M. In ref. 11, a 5-NI sample with a 10^{-7} M concentration was detected using the LSPR technique. Picric acid was detected with a 10^{-6} M concentration, while literature analysis showed from 10^{-5}–10^{-6} M,[44,46] to 10^{-9}–10^{-10} M,[43,45] (10^{-10} M is the lowest concentration detected so far in literature). Authors in both ref. 43 and 45 used the fabrication of substrates that are

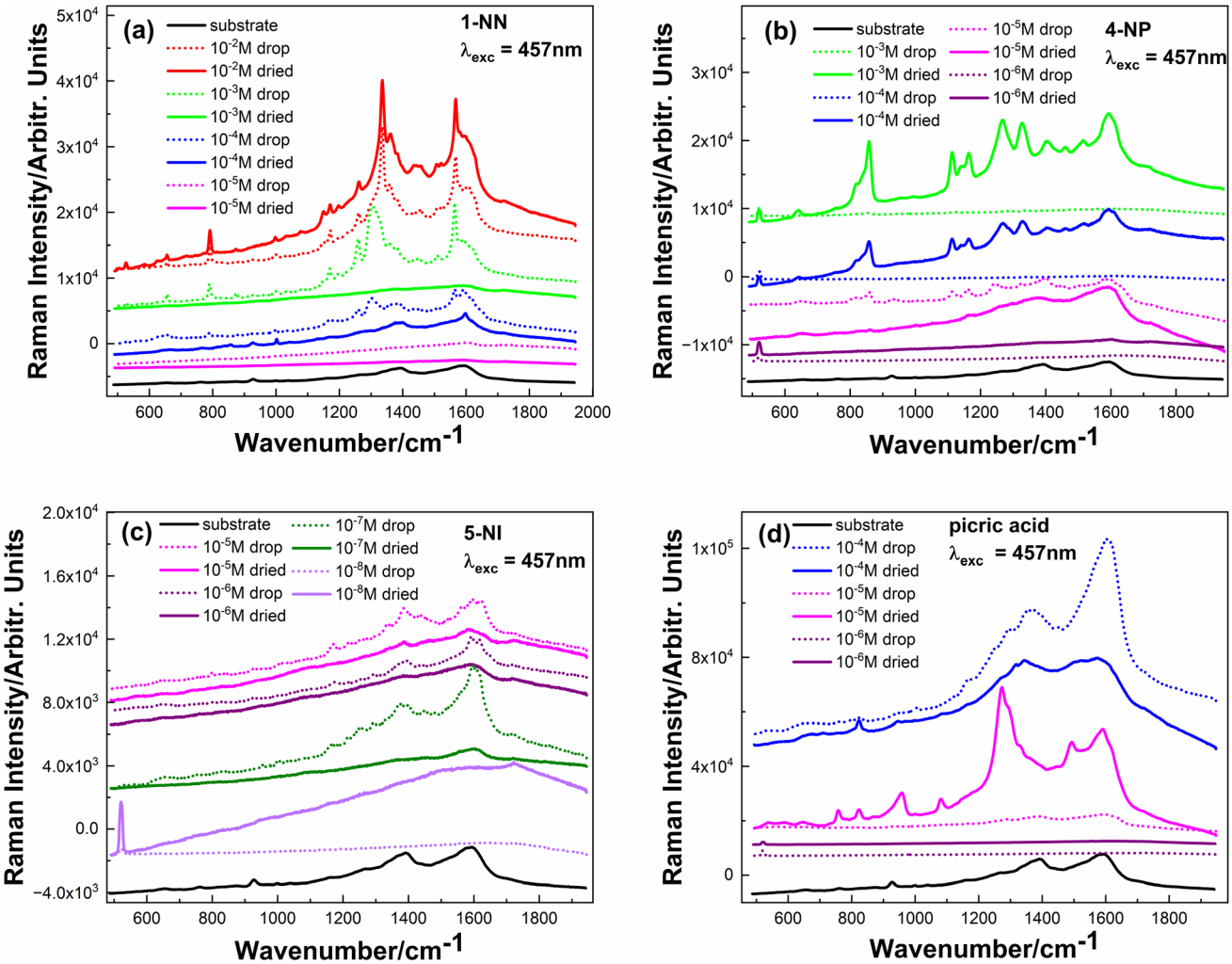

Fig. 5 SERS spectra of samples drop-casted on SiO_2 nanospheres covered with a 15 nm Ag layer: (a) 1-NN, (b) 4-NP, (c) 5-NI, and (d) picric acid. The measurement was performed on the drop of the solution immediately after its deposition (dotted curves) and after the solution was dried (solid curves).

formed with nanopillars using reactive ion etching. The 4-NP sample in our work was detected down to 10^{-5} M concentration. Different concentrations have been reported in the literature: 10^{-3} M,[41] 10^{-4} M,[39,40] 10^{-9} M,[38] (fabricated multihole capillaries covered with Au nanoparticles), and 10^{-12} M[38] (synthesized Ag nanospheres on ZnO multipods and used 532 nm laser excitation). 10^{-4} M concentration was detected for the 1-NN sample (there are no data in the literature at the moment).

For all investigated analytes, we calculated the enhancement factors of SERS, which are presented in Table 1.

The enhancement factor was calculated using the following formula:

Table 1 Enhancement factors for all investigated analytes, both with Ag NPs and on the SERS substrate, and the corresponding lowest concentrations detected (LOD). The vibrational modes used to determine EF are also specified

	With Ag NPs		On SiO_2 Ag 15 nm substrate	
Analyte	EF	LOD	EF	LOD
4NP	1343 cm^{-1}–1.5 × 10^2 1595 cm^{-1}–1.0 × 10^3	10^{-5} M	1595 cm^{-1}–3.0 × 10^3	10^{-5} M
5NI	1380 cm^{-1}–1.0 × 10^3	10^{-4} M	1380 cm^{-1}–6.7 × 10^5 1562 cm^{-1}–7.6 × 10^5	10^{-7} M
1NN	—	10^{-2} M	1568 cm^{-1}–4.0 × 10^2	10^{-4} M
Picric acid	1282 cm^{-1}–3.0 × 10^3	10^{-6} M	1282 cm^{-1}–3.7 × 10^4	10^{-5} M

$$\mathrm{EF} = \frac{I_{\mathrm{SERS}}/C_{\mathrm{SERS}}}{I_{\mathrm{Raman}}/C_{\mathrm{Raman}}},$$

where I_{SERS} – the intensity of the SERS band, I_{Raman} – the intensity of the Raman band, C_{SERS} – the concentration of molecule measured by SERS, and C_{Raman} – the concentration of molecule measured by Raman spectroscopy.

Conclusions

We investigated the possibility of detecting small concentrations of explosive materials using the SERS technique. Two approaches were used: mixing analyte molecules with silver nanoparticles and drop-casting those on Si substrates and drop-casting analytes fabricated using SERS substrates. SERS measurements allowed us to detect explosive materials by applying both approaches with the next limits of detection: 5-NI-10^{-7} M, picric acid-10^{-6} M, 4-NP-10^{-5} M, and 1-NN-10^{-4} M. The SERS enhancement factors vary from 1.5×10^2 to 7.6×10^5 depending on the analyte under study. Possible reasons for the different enhancements of the above analytes, as well as the differences in the liquid (drop) and dried states, are discussed in this study.

Data availability

All data supporting the findings of this study are included within the manuscript.

Author contributions

N. M.: investigation, project administration, writing – original draft, formal analysis. V. D.: conceptualization, methodology, supervision, formal analysis, writing – review and editing. O. K.: conceptualization, methodology. O. I.: investigation, formal analysis. P. D.: investigation, formal analysis. V. L.: investigation, formal analysis. V. C.: methodology, supervision. O. K.: methodology, supervision. V. Y.: supervision, writing – review and editing.

Conflicts of interest

The authors declare that they have no known competing financial interests or personal relationships that could have appeared to influence the work reported in this paper.

Acknowledgements

This work was funded by grant of the NAS of Ukraine to research laboratories/groups of young scientists no. 06/01-2024(5). The authors are grateful to M. A. Skoryk (I. M. Frantsevich Institute for Problems of Materials Science, National Academy of Sciences of Ukraine) for performing the SEM measurements.

References

1 D. O'Flynn, C. B. Reid, C. Christodoulou, M. D. Wilson, M. C. Veale, P. Seller, D. Hills, H. Desai, B. Wong and R. Speller, *J. Instrum.*, 2013, **8**, P03007.
2 A. N. Garroway, M. L. Buess, J. B. Miller, B. H. Suits, A. D. Hibbs, G. A. Barrall, R. Matthews and L. J. Burnett, *IEEE Trans. Geosci. Electron.*, 2001, **39**, 1108–1118.
3 K. E. Brown, M. T. Greenfield, S. D. McGrane and D. S. Moore, *Anal. Bioanal. Chem.*, 2016, **408**, 49–65.
4 J. S. Caygill, F. Davis and S. P. J. Higson, *Talanta*, 2012, **88**, 14–29.
5 H. A. Yu, J. Lee, S. W. Lewis and D. S. Silvester, *Anal. Chem.*, 2017, **89**, 4729–4736.
6 Y. Salinas, R. Martínez-Máñez, M. D. Marcos, F. Sancenón, A. M. Costero, M. Parra and S. Gil, *Chem. Soc. Rev.*, 2012, **41**, 1261–1296.
7 T. P. Forbes, E. Sisco and M. Staymates, *Anal. Chem.*, 2018, **90**, 6419–6425.
8 X. Sun, Y. Wang and Y. Lei, *Chem. Soc. Rev.*, 2015, **00**, 1–3.
9 C. Cheng, I. E. Kirkbride, D. N. Batchelder, R. J. Lacey and T. G. Sheldon, *J. Forensic Sci.*, 1995, **40**, 31.
10 I. Azuri, A. Hirsch, A. M. Reilly, A. Tkatchenko, S. Kendler, O. Hod and L. Kronik, *Beilstein J. Org. Chem.*, 2018, **14**, 381–388.
11 V. I. Chegel, A. M. Lopatynskyi, V. K. Lytvyn, P. V. Demydov, J. P. Martínez-Pastor, R. Abargues, E. A. Gadea and S. A. Piletsky, *Semicond. Phys., Quantum Electron. Optoelectron.*, 2020, **23**, 431–436.
12 E. Aznar-Gadea, P. J. Rodríguez-Canto, J. P. Martínez-Pastor, A. Lopatynskyi, V. Chegel and R. Abargues, *ACS Appl. Polym. Mater.*, 2021, **3**, 2960–2970.
13 L. Shi, L. Zhang and Y. Tian, *Analysis Sensing*, 2023, **3**, e202200064.
14 T. Moisoiu, M. P. Dragomir, S. D. Iancu, S. Schallenberg, G. Birolo, G. Ferrero, D. Burghelea, A. Stefancu, R. G. Cozan, E. Licarete, A. Allione, G. Matullo, G. Iacob, Z. Bálint, R. I. Badea, A. Naccarati, D. Horst, B. Pardini, N. Leopold and F. Elec, *Mol. Med.*, 2022, **28**, 39.
15 V. Moisoiu, S. D. Iancu, A. Stefancu, T. Moisoiu, B. Pardini, M. P. Dragomir, N. Crisan, L. Avram, D. Crisan, I. Andras, D. Fodor, L. F. Leopold, C. Socaciu, Z. Bálint, C. Tomuleasa, F. Elec and N. Leopold, *Colloids Surf., B*, 2021, **208**, 112064.
16 M. V. Chursanova, V. M. Dzhagan, V. O. Yukhymchuk, O. S. Lytvyn, M. Y. Valakh, I. A. Khodasevich, D. Lehmann, D. R. T. Zahn, C. Waurisch and S. G. Hickey, *Nanoscale Res. Lett.*, 2010, **5**, 403.
17 S. P. Usha, H. Manoharan, R. Deshmukh, R. Álvarez-Diduk, E. Calucho, V. V. R. Sai and A. Merkoçi, *Chem. Soc. Rev.*, 2021, **50**, 13012–13089.
18 R. E. Ionescu, E. N. Aybeke, E. Bourillot, Y. Lacroute, E. Lesniewska, P. M. Adam and J. L. Bijeon, *Sensors*, 2017, **17**, 236.

19 L. Mikoliunaite, R. D. Rodriguez, E. Sheremet, V. Kolchuzhin, J. Mehner, A. Ramanavicius and D. R. T. Zahn, *Sci. Rep.*, 2015, **5**, 13150.
20 V. Lughi, A. Bonifacio, M. Barbone, L. Marsich and V. Sergo, *J. Nanopart. Res.*, 2013, **15**, 1663.
21 A. Muravitskaya, A. Rumyantseva, S. Kostcheev, V. Dzhagan, O. Stroyuk and P.-M. Adam, *Opt. Express*, 2016, **24**, 168–A173.
22 E. Beleites, C. Byrne, H. J. Chiadò, A. Chis, M. Chisanga, M. Daniel, A. Dybas, J. Eppe, G. G. Falgayrac, K. Faulds, H. Gebavi, F. Giorgis, R. Goodacre, D. Graham, P. La Manna, S. Laing, L. Litti, F. M. Lyng, K. Malek, C. Malherbe, M. P. M. Marques, M. Meneghetti, E. Mitri, V. Mohaček-Grošev, C. Morasso, H. Muhamadali, P. Musto, C. Novara, M. Pannico, G. Penel, O. Piot, T. Rindzevicius, E. A. Rusu, M. S. Schmidt, V. Sergo, G. D. Sockalingum, V. Untereiner, R. Vanna, E. Wiercigroch and A. Bonifacio, *Anal. Chem.*, 2020, **92**, 4053–4064.
23 H. Aitchison, J. Aizpurua, H. Arnolds, J. Baumberg, S. Bell, A. Bonifacio, R. Chikkaraddy, P. Dawson, B. De Nijs, V. Deckert, I. Delfino, G. Di Martino, O. Eremina, K. Faulds, A. Fountain, S. Gawinkowski, M. Gomez Castano, R. Goodacre, J. Gracie, D. Graham, J. Guicheteau, L. Hardwick, M. Hardy, C. Heck, L. Jamieson, M. Kamp, A. Keeler, C. Kuttner, J. Langer, S. Mahajan, N. Martín Sabanés, K. Murakoshi, M. Porter, G. Schatz, S. Schlücker, Z. Tian, A. Tripathi, R. Van Duyne and P. Vikesland, *Faraday Discuss.*, 2017, **205**, 561–600.
24 D. B. Grys, B. de Nijs, J. Huang, O. A. Scherman and J. J. Baumberg, *ACS Sens.*, 2021, **6**, 4507–4514.
25 T. Itoh, M. Procházka, Z. C. Dong, W. Ji, Y. S. Yamamoto, Y. Zhang and Y. Ozaki, *Chem. Rev.*, 2022, **123**, 1552–1634.
26 J. Langer, D. J. de Aberasturi, J. Aizpurua, R. A. Alvarez-Puebla, B. Auguié, J. J. Baumberg, G. C. Bazan, S. E. J. Bell, A. Boisen, A. G. Brolo, J. Choo, D. Cialla-May, V. Deckert, L. Fabris, K. Faulds, F. Javier García de Abajo, R. Goodacre, D. Graham, A. J. Haes, C. L. Haynes, C. Huck, T. Itoh, M. K. Kneipp, N. A. Kotov, H. Kuang, E. C. Le Ru, H. K. Lee, J.-F. Li, X. Y. Ling, S. A. Maier, T. Mayerhöfer, M. Moskovits, K. Murakoshi, J.-M. Nam, S. Nie, Y. Ozaki, I. Pastoriza-Santos, J. Perez-Juste, J. Popp, A. Pucci, S. Reich, B. Ren, G. C. Schatz, T. Shegai, S. Schlücker, L.-L. Tay, K. G. Thomas, Z.-Q. Tian, R. P. Van Duyne, T. Vo-Dinh, Y. Wang, K. A. Willets, C. Xu, H. Xu, Y. Xu, Y. S. Yamamoto, B. Zhao and L. M. Liz-Marzán, *ACS Nano*, 2020, **14**, 28–117.
27 N. Chauhan, K. Saxena, R. Rawal, L. Yadav and U. Jain, *Prog. Biophys. Mol. Biol.*, 2023, **184**, 32–41.
28 D. Li, W. Yue, P. Gao, T. Gong, C. Wang and X. Luo, *TrAC, Trends Anal. Chem.*, 2024, **170**, 117426.
29 L. Szabó, L. F. Leopold, B. I. Cozar, N. Leopold, K. Herman and V. Chiș, *Cent. Eur. J. Chem.*, 2011, **9**, 410–414.
30 S. Almaviva, F. Artuso, I. Giardina, A. Lai and A. Pasquo, *Sensors*, 2022, **22**, 8338.
31 F. Zapata, M. López-López and C. García-Ruiz, *Appl. Spectrosc. Rev.*, 2016, **51**(3), 227–262.
32 A. Hakonen, P. O. Andersson, M. S. Schmidt, T. Rindzevicius and M. Käll, *Anal. Chim. Acta*, 2015, **893**, 1–13.
33 R. Gillibert, J. Qi Huang, Y. Zhang, W. L. Fu and M. L. de La Chapelle, *TrAC, Trends Anal. Chem.*, 2018, **105**, 166–172.
34 C. Muehlethaler, M. Leona and J. R. Lombardi, *Anal. Chem.*, 2016, **88**, 152–169.
35 W. J. Peveler, S. B. Jaber and I. P. Parkin, *Forensic Sci., Med., Pathol.*, 2017, **13**, 490–494.
36 K. C. To, S. Ben-Jaber and I. P. Parkin, *ACS Nano*, 2020, **14**, 10804–10833.
37 Z. I. Kazantseva, I. A. Koshets, A. V. Mamykin, A. S. Pavluchenko, O. L. Kukla, A. A. Pud, N. A. Ogurtsov, Y. V. Noskov, R. V. Rodik and S. G. Vyshnevskyy, *Semicond. Phys., Quantum Electron. Optoelectron.*, 2023, **26**, 332–342.
38 M. K. K. Oo, Y. Guo, K. Reddy, J. Liu and X. Fan, *Anal. Chem.*, 2012, **84**, 3376–3381.
39 H. Bao, H. Zhang, L. Zhou, G. Liu, Y. Li and W. Cai, *Langmuir*, 2017, **33**, 12934–12942.
40 D. A. Perry, H. J. Son, J. S. Cordova, L. G. Smith and A. S. Biris, *J. Colloid Interface Sci.*, 2010, **342**, 311–319.
41 M. T. Alula, P. Lemmens, M. Madiba and B. Present, *Cellulose*, 2020, **27**, 2279–2292.
42 E. A. Kumar, N. R. Barveen, T.-J. Wang, T. Kokulnathan and Y.-H. Chang, *Microchem. J.*, 2021, **170**, 106660.
43 A. Hakonen, F.-C. Wang, P. O. Andersson, H. Wingfors, T. Rindzevicius, M. S. Schmidt, V. R. Soma, S. Xu, Y. Li, A. Boisen and H.-A. Wu, *ACS Sens.*, 2017, **2**, 198–202.
44 S. S. B. Moram, C. Byram and V. R. Soma, *Bull. Mater. Sci.*, 2020, **43**, 53.
45 A. Hakonen, K. Wu, M. S. Schmidt, P. O. Andersson, A. Boisen and T. Rindzevicius, *Talanta*, 2018, **189**, 649–652.
46 C. Byram, S. S. B. Moram, A. K. Shaik and V. R. Soma, *Chem. Phys. Lett.*, 2017, **685**, 103–107.
47 W. Stöber, A. Fink and D. E. Bohn, *J. Colloid Interface Sci.*, 1968, **26**, 62–69.
48 V. Dzhagan, N. Mazur, O. Kapush, M. Skoryk, Y. Pirko, A. Yemets, V. Dzhahan, P. Shepeliavyi, M. Valakh and V. Yukhymchuk, *ACS Omega*, 2024, **9**, 4819–4830.
49 V. M. Dzhagan, Y. V. Pirko, A. Y. Buziashvili, S. G. Plokhovska, M. M. Borova, A. I. Yemets, N. V. Mazur, O. A. Kapush and V. O. Yukhymchuk, *Ukr. J. Phys.*, 2022, **67**, 80–87.
50 Y. L. Mikhlin, S. A. Vorobyev, S. V. Saikova, E. A. Vishnyakova, A. S. Romanchenko, S. M. Zharkov and Y. V. Larichev, *Appl. Surf. Sci.*, 2018, **427**, 687.
51 P. V. Demydov, A. M. Lopatynskyi, I. I. Hudzenko and V. I. Chegel, *Semicond. Phys., Quantum Electron. Optoelectron.*, 2021, **24**, 304–311.
52 S. Mukherji, S. Bharti, G. Shukla and S. Mukherji, *Phys. Sci. Rev.*, 2018, 20170082.
53 N. V. Mazur, O. A. Kapush, O. F. Isaieva, S. I. Budzulyak, A. Y. Buziashvili, Y. V. Pirko, M. A. Skoryk, A. I. Yemets, O. M. Hreshchuk, V. O. Yukhymchuk, V. M. Dzhagan and F. K. T. TilaPhys, *Chem. Solid State*, 2023, **24**, 682–691.
54 V. Dzhagan, O. Smirnov, M. Kovalenko, O. Gudymenko, N. Mazur, O. Kapush, M. Skoryk, Y. Pirko, A. Yemets, M. Valakh, P. Shepeliavyi and V. Yukhymchuk, *Anal. Biochem.*, 2023, **681**, 115328.

55 R. Rastogi, E. A. D. Foli, R. Vincent, P.-M. Adam and S. Krishnamoorthy, *ACS Appl. Mater. Interfaces*, 2021, **13**, 32653–32661.
56 O.-M. Buja, O. D. Gordan, N. Leopold, A. Morschhauser, J. Nestler and D. R. T. Zahn, *Beilstein J. Nanotechnol.*, 2017, **8**, 237–243.
57 A. M. Figat, B. Bartosewicz, M. Liszewska, B. Budner, M. Norek and B. J. Jankiewicz, *Langmuir*, 2023, **39**, 8646–8657.
58 V. Chegel, O. Rachkov, A. Lopatynskyi, S. Ishihara, I. Yanchuk, Y. Nemoto, J. P. Hill and K. Ariga, *J. Phys. Chem. C*, 2012, **116**, 2683–2690.
59 A. Stefancu, S. D. Iancu and N. Leopold, *J. Phys. Chem. C*, 2021, **125**, 12802–12810.
60 S. D. Iancu, A. Stefancu, V. Moisoiu, L. F. Leopold and N. Leopold, *Beilstein J. Nanotechnol.*, 2019, **10**, 2338–2345.
61 D. C. Rodrigues, M. L. Souza, K. S. Souza, D. P. dos Santos, G. F. S. Andrade and M. L. A. Temperini, *Phys. Chem. Chem. Phys.*, 2015, **17**, 21294–21301.
62 Y.-C. Chang, M. M. Dvoynenko, H. Ke, H.-H. Hsiao, Y.-L. Wang and J.-K. Wang, *J. Phys. Chem. C*, 2021, **125**, 27267–27274.
63 A. Mukherjee, F. Wackenhut, A. Dohare, A. Horneber, A. Lorenz, H. Müchler, A. J. Meixner, H. A. Mayer and M. Brecht, *J. Phys. Chem. C*, 2023, **127**, 13689–13698.
64 M. Rahaman, A. G. Milekhin, A. Mukherjee, E. E. Rodyakina, A. V. Latyshev, V. M. Dzhagan and D. R. T. Zahn, *Faraday Discuss.*, 2019, **214**, 309–323.
65 R. E. Ionescu., E. N. Aybeke, E. Bourillot, Y. Lacroute, E. Lesniewska, P.-M. Adam and J.-L. Bijeon, *Sensors*, 2017, **17**, 236.
66 A. Mukherjee, Q. Liu, F. Wackenhut, F. Dai, M. Fleischer, P.-M. Adam, A. J. Meixner and M. Brecht, *Molecules*, 2022, **27**, 5097.
67 R. Rastogi, H. Arianfard, D. Moss, S. Juodkazis, P.-M. Adam and S. Krishnamoorthy, *ACS Appl. Mater. Interfaces*, 2021, **13**, 9113–9121.
68 I. Izquierdo-Lorenzo, S. Jradi and P.-M. Adam, *RSC Adv.*, 2014, **4**, 4128.
69 V. A. Dan'ko, I. Z. Indutnyi, V. I. Mynko, P. M. Lytvyn, M. V. Lukaniuk, H. V. Bandarenka, A. L. Dolgyi and S. V. Redko, *Semicond. Phys., Quantum Electron. Optoelectron.*, 2021, **24**, 48–55.